



Sulfonated and gamma-irradiated waste expanded polystyrene with iron oxide nanoparticles, for removal of indigo carmine dye in textile wastewater



Cristina A. De León-Condés^a, Gabriela Roa-Morales^b, Gonzalo Martínez-Barrera^{c,*},
Carmina Menchaca-Campos^d, Bryan Bilyeu^e, Patricia Balderas-Hernández^b,
Fernando Ureña-Núñez^f, Helen Paola Toledo-Jaldin^a

^a Posgrado en Materiales, Facultad de Química, Universidad Autónoma del Estado de México, Paseo Colon esquina Paseo Tollocan S/N, 50180, Toluca, Mexico

^b Centro Conjunto de Investigación en Química Sustentable, Universidad Autónoma del Estado de México - Universidad Nacional Autónoma de México (UAEM-UNAM), Carretera Toluca-Atacomulco, km 14.5, Unidad El Rosedal, C.P. 50200, Mexico

^c Laboratorio de Investigación y Desarrollo de Materiales Avanzados (LIDMA), Facultad de Química, Universidad Autónoma del Estado de México, Km.12 de la carretera Toluca-Atacomulco, San Cayetano, 50200, Mexico

^d Centro de Investigación en Ingeniería y Ciencias Aplicadas (CIICAp), Universidad Autónoma del Estado de Morelos (UAEM), Av. Universidad 1001, Col. Chamilpa, C.P. 62209, Cuernavaca Morelos, Mexico

^e Department of Chemistry, Xavier University of Louisiana, Drexel Drive, Box 22, New Orleans, LA, 70125, USA

^f Instituto Nacional de Investigaciones Nucleares, Carretera México-Toluca S/N, 52750, La Marquesa Ocoyoacac, Mexico

ARTICLE INFO

Keywords:

Environmental science
Analytical chemistry
Materials chemistry
Physical chemistry
Materials science
Nanotechnology
Waste expanded polystyrene
Gamma radiation
Sulfonation
Textile wastewater
Indigo carmine dye
Fenton process

ABSTRACT

In this work, waste expanded polystyrene (WEPS) was irradiated with gamma rays, ranging doses from 100 kGy to 1,000 kGy. After irradiation, the WEPS had decrease on its glass transition temperature (T_g), as consequence of the scissions of its polymer chains. Then, the irradiated WEPS was sulfonated, and its degree of sulfonation (DS) was measured. The highest DS value, 46.6%, was obtained for an irradiation dose of 200 kGy. The sulfonated and irradiated polystyrene (denominated as iS-WEPS), was used as a support of iron oxide nanoparticles. Such composite system was denominated (FeO-NPs + iS-WEPS). The results show nanoparticle sizes of 31.5 nm containing 21.97% iron oxide. The composites followed a pseudo-second order model, with a maximum adsorption capacity of 20 mg/g, and an equilibrium time of 30 min, according to the Langmuir model. Moreover, the optimal conditions followed by the Fenton process were: pH = 3.2, H₂O₂ concentration = 0.32 mM/L, composite concentration (FeO-NPs + iS-WEPS) = 2 g/L, and a reaction time 20 min. Finally, 99% removal of indigo carmine dye was achieved, and a reduction of 83% of COD in textile wastewater.

1. Introduction

The daily produced wastewater by the textile industry are among the most polluting. These contain organic toxic compounds, which affect living beings (Aljeboree et al., 2017; Sanmuga and Senthamil, 2017). Textile wastewater treatments do not follow a generalized process for all kind of effluents, because this depends on the type of pollutants; whereby, combination of different methods is necessary; the physical, chemical, biochemical, and hybrid processes are the most used, but avoiding having high costs (Holkar et al., 2016). One alternative is the Fenton chemistry process, which has been widely proved on the degradation of hazardous organic compounds, dyes and industrial waste (Grisales et al., 2019). Such process is based on the Fe²⁺-H₂O₂ reaction,

which produces hydroxyl radicals by means of the oxidation of organic and inorganic compounds (Babuponnusami and Muthukumar, 2012; Hartmann et al., 2010). Moreover, in the heterogeneous Fenton process, iron reacts through to a solid support, such as zeolites, ion exchange resins or clay and carbon. In such procedure no sludge is produced (Liu et al., 2017).

Supported or unsupported metals or metal oxide nanoparticles are employed as heterogeneous Fenton catalysts (Espinosa et al., 2018). The oxide nanoparticles are produced by green methods; which have some advantages as, be safe, eco-friendly, low cost, and mainly do not use harmful compounds (Fahmy et al., 2018). In recent works, a high degree of sulfonation has been obtained for waste expanded polystyrene (WEPS), after submitting to ionizing radiation. Such improvement is due

* Corresponding author.

E-mail address: gonzomartinez02@yahoo.com.mx (G. Martínez-Barrera).

<https://doi.org/10.1016/j.heliyon.2019.e02071>

Received 26 March 2019; Received in revised form 8 May 2019; Accepted 8 July 2019

2405-8440/© 2019 The Author(s). Published by Elsevier Ltd. This is an open access article under the CC BY-NC-ND license (<http://creativecommons.org/licenses/by-nc-nd/4.0/>).

to the cross-linking of their polymer chains. Moreover, WEPS has been used for removal of contaminants in wastewater (Haryono and Harmami, 2012; Tabekh et al., 2015).

In this work, iron oxides nanoparticles were obtained using green tea extracts; then they supported irradiated and sulfonated waste expanded polystyrene (iS-WEPS). Such composites (denominated as FeO-NPs + iS-WEPS), were used as a heterogeneous Fenton catalyst, for removal of indigo carmine dye in textile wastewater. Moreover, the adsorption isotherms and kinetics, as well as chemical oxygen demand (COD), were studied.

2. Material and methods

2.1. Reagents

For the calculation of the degree of sulfonation the following reagents were employed: sulfuric acid (96.8 g/dl), HCl, NaCl and NaOH (analytical grade, Sigma-Aldrich Chemicals). For the green synthesis were used: commercial grade green tea (Herbacil™), and ferrous salt (FeCl₂ · 4H₂O) (analytical grade, Sigma-Aldrich Chemicals). For the Fenton process, H₂O₂ 30% solution (analytical grade, Fermont), was used. Finally, indigo carmine dye (Sigma Aldrich BSC Code ACL-18, Mw = 466 g/mol), was used for the isotherms and the adsorption kinetics tests.

2.2. Gamma irradiation of waste expanded polystyrene (iWEPS)

Waste expanded polystyrene (WEPS) was washed, dried and crushed for to obtain pieces of size 0.3–0.5 cm²; then these were exposed at different gamma irradiation doses (100, 200, 400, 600, 800 and 1,000 kGy), at a dose rate of 3.5 kGy/h, remained in air at room temperature. The samples were denominated as iWEPS. Irradiation process was carried out in a Transelektro Irradiator LGI01 with a ⁶⁰Co source; manufactured by IZOTOP Institute of Isotopes Co. Ltd. (Budapest, Hungary), and located at the National Institute of Nuclear Research (ININ, México).

2.3. Sulfonation of irradiated waste expanded polystyrene (iS-WEPS)

The iWEPS samples were sulfonated following the optimized method reported by De-León et al. (2019) (De León-Condés et al., 2019). This consist in mixing 7.5g of irradiated waste expanded polystyrene with 100 mL of H₂SO₄ (96%), and to kept it under agitation for 30 min at 95 °C (Fig. 1). Finally, the iS-WEPS is separated from the solution by filtration and then washed.

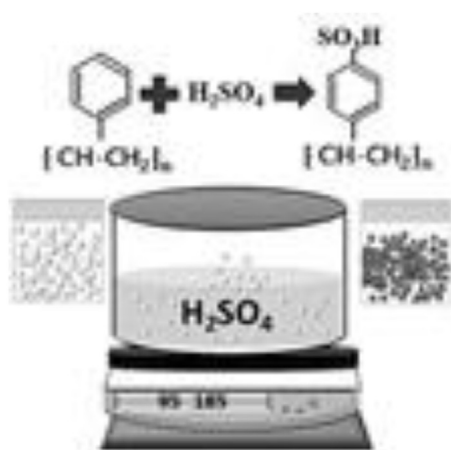


Fig. 1. Schematic illustration of the sulfonation process of irradiated waste expanded polystyrene (iWEPS).

2.4. Elaboration of the composite (FeO-NPs + iS-WEPS)

The composites elaboration consisted first in obtaining the iron nanoparticles (mixing a ferrous solution (FeCl₂·4H₂O) 0.1M and 150 mL of deionized water; under a nitrogen atmosphere). Previously, green tea extracts were obtained by mixing 13g of green tea (Herbacil™) and 500 mL of deionized water, stirred at 80 °C and vacuum-filtered. Then, the solutions had 2:3 ratio of ferrous solution:green tea, which was stirred during 60 min (Shahwan et al., 2011). Finally, 9g of iS-WEPS was added, and the final mixture was stirred for 1h at 24 °C, for to obtain the composite (FeO-NPs + iS-WEPS).

2.5. Characterization of the materials

The glass transition temperature of WEPS and iWEPS were measured in a TGA-DSC equipment (Netzsch STA 449 F3 Jupiter), with a heating speed of 10 °C/min, in nitrogen atmosphere. While the iWEPS was analyzed by Fourier transform infrared spectroscopy (FT-IR) in a spectrophotometer, equipped with an accessory for measuring of Attenuated Total Reflectance (ATR). After the sulfonation process, the degree of sulfonation of the irradiated and sulfonated polystyrene (iS-WEPS) was calculated, according to (De León-Condés et al., 2019; Zaidi, 2003).

The iron oxide nanoparticles sizes were determined by transmission electron microscopy (TEM), from carbon-coated evaporated drops, using a JEOL 2100 microscope at 200 kV, with a LaB₆ source. The nanoparticles sizes were measured using the ImageJ software by counting at least 1,000 nanoparticles on each TEM image. Finally, the composites (FeO-NPs + iS-WEPS) were characterized by: a) X-ray powder diffraction (XRD) using a XRD Rigaku/Ultima-IV equipment with Cu- α radiation (1.5406 Å) at 45 kV and scanning speed of 2°/min, and b) scanning electron microscopy (SEM), using a JEOL-5900-LV microscope, at 20 keV in high-vac mode (with gold sputtering). Such equipment includes an energy dispersive X-ray probe for semi-quantitative elemental analysis.

2.6. Adsorption isotherms and kinetics

The kinetic experiments were performed for determination of the equilibrium time. For this, 100 mg of the composite (FeO-NPs + iS-WEPS) was mixed with 50 mL of indigo carmine dye solution (50 mg/L, as initial concentration); such aqueous samples were measured every 5 minutes until 50 minutes for to find the equilibrium time. Then, the samples were centrifuged and decanted. The kinetics adsorption process was studied by three methods: pseudo-first order, pseudo-second order, and Elovich.

The adsorption isotherm experiments were carried out with an indigo carmine dye solution. For this, were prepared beakers with 50 mg of adsorbent and 25 mL of indigo carmine solution (10–80 mg/L) at pH 3.2. The beakers were sealed and stirred for 30 min, at room temperature. After stirring, the indigo carmine concentration in the solution was measured by using a UV-Vis spectrophotometer Perkin-Elmer Model Lambda 25. Moreover, Langmuir, Freundlich and Langmuir-Freundlich models, as well as Origin 8.0 software were used for the analysis of the adsorption isotherms. The concentration of indigo carmine at equilibrium, q_e (mg/g), in the adsorbent samples, was calculated by Eq. (1):

$$q_e = \frac{(C_0 - C_e)V}{W} \quad (1)$$

where C_0 and C_e (mg/L) are the liquid phase concentrations of indigo carmine at initial and equilibrium, respectively; V is the volume of the solution (L), and W is the mass of the adsorbent (g).

2.7. Textile wastewater with the composites (FeO-NPs+iS-WEPS)

Textile wastewater samples were collected from a textile workshop located in México, in plastic containers and cooled down to 4 °C, then

they were transported to the laboratory for their treatment and analysis. The samples were subjected to sedimentation for 5 h, in order to separate the solids, such as cotton threads. The removal was performed in a beaker under magnetic stirring at 60 rpm and room temperature.

The pH of the wastewater samples was 6.7 (measured with a pH M210 Meter). The concentration of indigo carmine dye was 64.6 mg/L (measured with a UV-vis spectrophotometer). While the COD value was 2,422 mg/L, it was measured according to the open reflux method of the American Public Health Association (APHA).

The mixtures containing textile wastewater (100 mL) and the composites (FeO-NPs + iS-WEPS) (0.1g), were tested at different concentrations of hydrogen peroxide. The results showed that pH decrease (from 6.7 to 3.2) after adding the composites, due to the natural acidity of these. The pH value of 3.2 is similar to that reported for textile wastewater after removing indigo carmine dye, following a Fenton process (Al-Sabagh et al., 2018; Babuponnusami and Muthukumar, 2012; Gutiérrez-Segura et al., 2009; Zaied et al., 2011).

3. Results and discussion

3.1. FT-IR spectroscopy of the (WEPS) and (iWEPS)

The FT-IR spectrum of the WEPS is shown in Fig. 2. The main absorption bands are located at 3025 cm^{-1} corresponding to aromatic C-H stretching; at 2921 cm^{-1} attributed to symmetrical and asymmetrical stretching vibration of CH_2 ; at 1600, 1499 and 1442 cm^{-1} corresponding to the C-C stretching bands for aromatic ring, however, the band at 1442 cm^{-1} may result from the ring breathing of the deformation vibration of CH_2 ; and finally at 1018, 757 and 700 cm^{-1} , corresponding to the =C-H stretching for aromatic ring (Olmos et al., 2014; Yabagi et al., 2018).

The FT-IR spectra of the irradiated WEPS are shown in Fig. 2. They do not show different peaks respect to non-irradiated ones. Thus, no new chemical bonds were produced after irradiation.

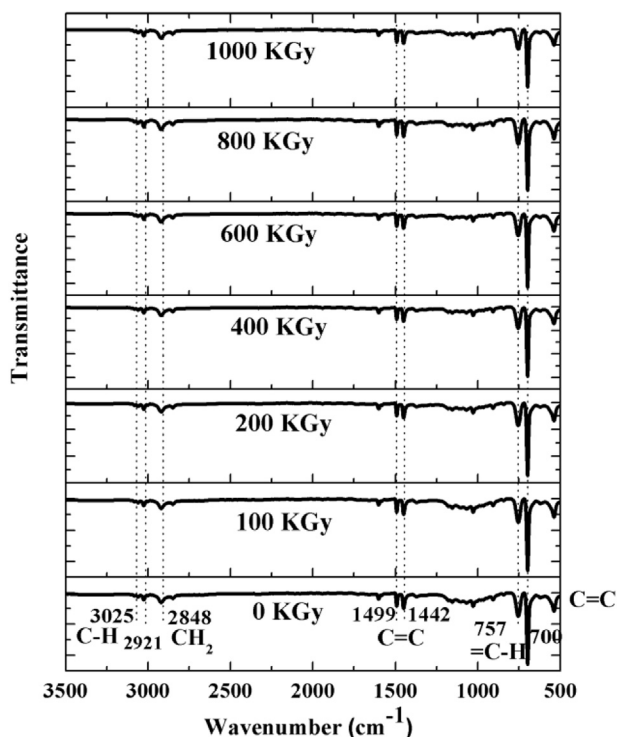


Fig. 2. FT-IR spectra of non-irradiated WEPS, and irradiated WEPS.

3.2. Glass transition temperature of the (WEPS) and (iWEPS)

The differential scanning calorimetry (DSC) analysis was carried out, in order to obtain the glass transition temperature (T_g) (Fig. 3). The results show the T_g at 103 °C for non-irradiated WEPS, and at 98.1 °C for WEPS irradiated at 200 kGy. Such diminution on the temperature is result of the molecular weight decrease, caused by the scissions of the polymer chains (Spadaro et al., 2017; Yousif and Haddad, 2013) (Correño-Alonso and Mendez-Bautista, 2010).

3.3. Degree of sulfonation of the (iWEPS)

The degree of sulfonation of non-irradiated (WEPS), and irradiated waste expanded polystyrene (iWEPS), is shown in Fig. 4. Two well-defined behaviors are obtained: a) The degree of sulfonation increase when the radiation dose increase, up to 200 kGy. This can be attributed to the scission of the polymer chains, that favor the sulfonation process. The value for non-irradiated WEPS was 23.5%, while that for irradiated at 200 kGy was 46.6%. This means an improvement of 50%; b) At doses higher than 200 kG, the degree of sulfonation gradually decrease, up to 8.8%, which could be attributed to a greater scission of the polymer chains.

3.4. Crystallinity of the iron oxide nanoparticles (FeO-NPs)

The crystallinity of the iron oxide nanoparticles is shown in Fig. 5. The crystalline phases are: i) α Fe_2O_3 , ii) β Fe_2O_3 , iii) γ Fe_2O_3 , iv) ϵ Fe_2O_3 , v) Fe_3O_4 and vi) FeO. Their respective crystalline planes are shown in the same Fig. 5 (Crane and Scott, 2012; Cui et al., 2013; Guivar et al., 2014; Liu et al., 2016; Pandey et al., 2014).

3.5. Morphological characterization of the composites (FeO-NPs+iS-WEPS)

The TEM image of the composite (FeO-NPs + iS-WEPS) is shown in Fig. 6a. Quasi spherical nanoparticles are observed. They show an uniform distribution of diameter sizes, ranging from 5 to 80 nm (Fig. 6b), with an average diameter size of 31.5 nm, and a standard deviation, $\sigma = 0.30$. Such diameters are higher than those for non-irradiated and sulfonated WEPS, reported in a previous work by the authors, namely 25.5 nm, with $\sigma = 0.44$ (De León-Condés et al., 2019). Thus, gamma irradiation generates agglomeration of NPs and growth of crystalline grains. These irradiated NPs, have similar diameter sizes than those obtained when polyphenols are used (Fahmy et al., 2018).

Fig. 7a shows a SEM image of the composite (FeO-NPs + iS-WEPS). A rough surface with detached particles and some channels (shown inside the circle), are observed. The presence of channels increase the

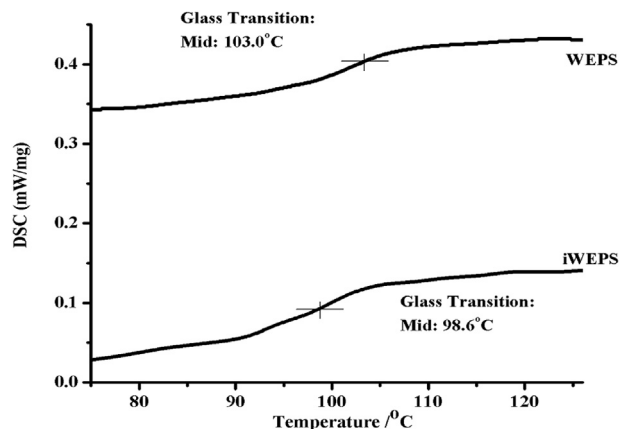


Fig. 3. DSC curves of the (WEPS) and (iWEPS).

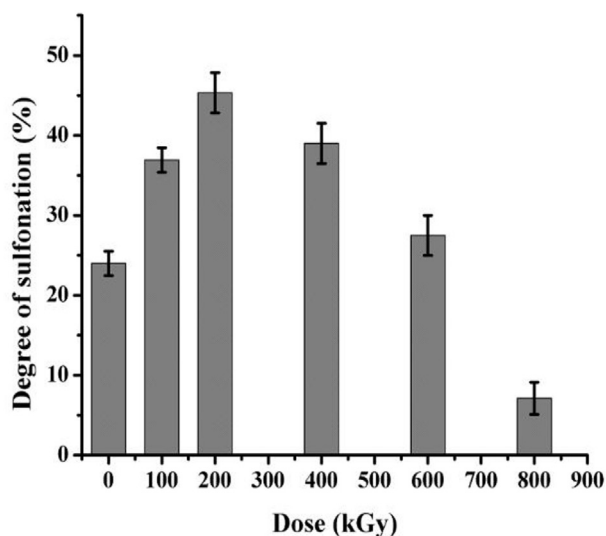


Fig. 4. Degree of sulfonation of non-irradiated and irradiated WEPS.

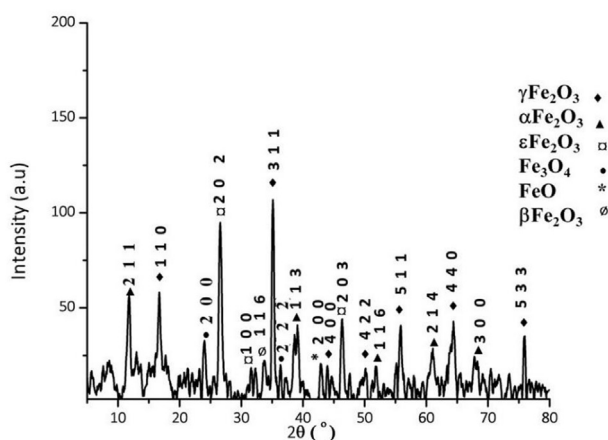


Fig. 5. X-ray diffraction spectrum of the iron oxide nanoparticles.

superficial area, which promote the adsorption process (Tai et al., 2016). The surface morphology after irradiation is very different to that for non-irradiated and sulfonated WEPS, reported in a previous work by the authors, where a smooth and homogeneous surface with some voids was obtained (De León-Condés et al., 2019). Thus, gamma irradiation produces modifications on the surface of the composite, mainly those due to

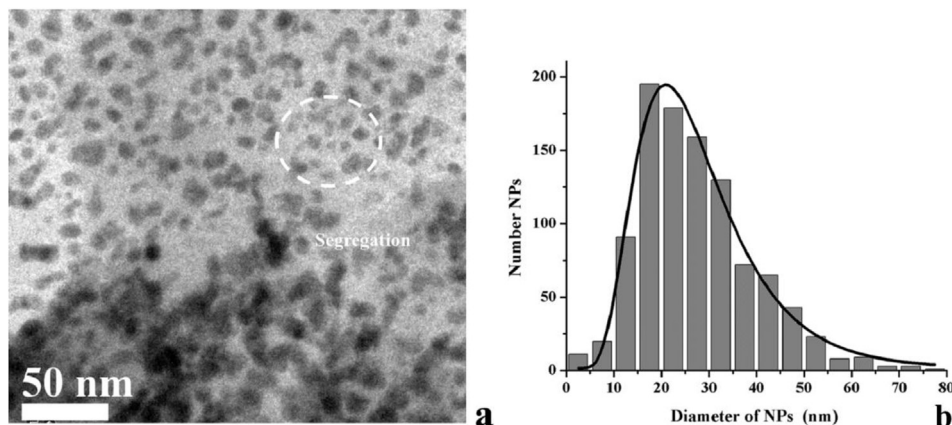


Fig. 6. TEM image of the composite (FeO-NPs + iS-WEPS) (a), and their distribution of diameter sizes (b).

the scission of the polymer chains. The composition of the composite was analyzed by EDS (Fig. 7b). The chemical elements detected were: O (36.77%), C (27.9%), Fe (21.97%), and S (12.56%). They are constituents of the green tea molecules, as well as of the FeO nanoparticles, corroborate by the oxygen presence (Wang et al., 2014).

3.6. Kinetics and adsorption isotherms

The equilibrium time was obtained at 30 min (Fig. 8a), with 60% removal of indigo carmine dye (Fig. 8b). The parameters for each model are shown in Table 1. The experimental data are agreeing with those for the pseudo-first or pseudo-second order models, as it is shown in Fig. 8a. Moreover, the correlation coefficients are higher for the pseudo-second order model than those for the first-order. According to the models, the adsorption occurs by chemisorption, with exchange of electrons between the composite (FeO-NPs + iS-WEPS) and the indigo carmine dye (Blanco-Flores et al., 2014). Thus, the adsorption process is carried out by chemical bonds between the adsorbent and adsorbate. Unfortunately, the Elovich model did not provided a good fit, thus the data are not shown.

Data for Freundlich and Langmuir models are shown in Fig. 9a and b, and in Table 2. According to the regression coefficient, the Freundlich model is better for describing the adsorption process of the composite (FeO-NPs + iS-WEPS); this has a monosurface of adsorption with a heterogeneous distribution of energy points, and interactions between adsorbed molecules (Liu et al., 2016). In addition, the maximum adsorption capacity of the composite was 20 mg/g, with $R^2 = 0.955$, obtained by the Langmuir model.

Lower values than 1.0 for the $1/n$ parameter, means that the adsorption is adequate; such parameter shows the relative distribution of the energy sites, which depend directly on the nature and strength of the adsorption process (Blanco-Flores et al., 2016). The interaction mechanism between the composite (FeO-NPs + iS-WEPS) and the indigo carmine dye, is based on the $-\text{SO}_3\text{H}$ groups, which generate strong electrostatic interactions with the dye molecules; while functional groups of the dyes create positive dipoles (Yu et al., 2017).

3.7. Heterogeneous Fenton process

Colored wastewater has a wide range of initial pH values, which is an important parameter that affects the removal efficiency in the Fenton processes. It have been reported pH values between 2 and 3 for removal of contaminants, when the homogeneous Fenton process is applied (Domenech et al., 2004; Nidheesh et al., 2013; Tai et al., 2016). At pH less than 3.5, Fe^{3+} controls the balance and the Fenton process is responsible for the elimination of the contaminant. But, at pH = 3.5 or higher, the solubility is controlled by the compound $\text{Fe}(\text{OH})_3$, and the removal of contaminants is due to a coagulation process and not to a

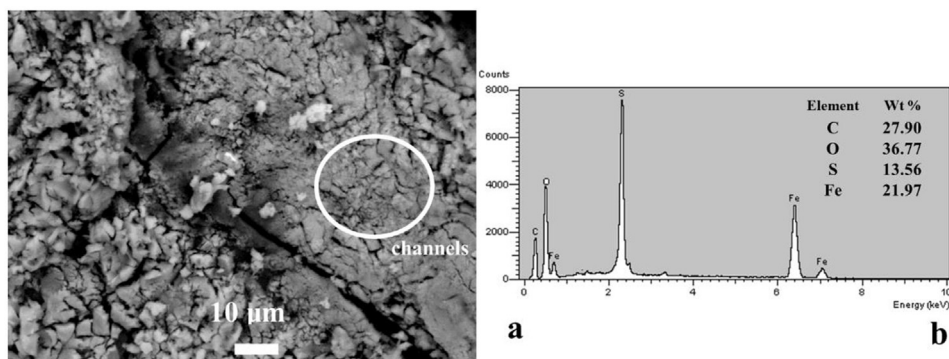


Fig. 7. SEM image of the composite (FeO-NPs + iS-WEPS) (a); and its chemical elements, obtained by EDS (b).

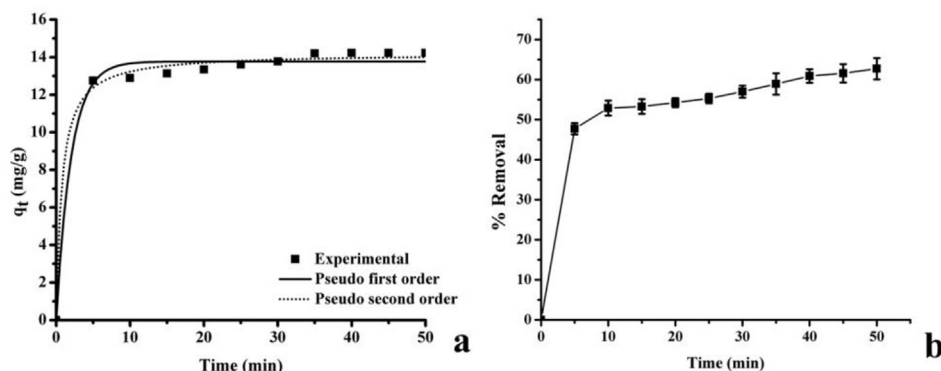


Fig. 8. Adsorption kinetics for removal of indigo carmine dye: pseudo-first and pseudo second order models (a); Removal percentage (b). Adsorbent dose = 2 g/L, volume of sample = 50 mL.

Table 1
Kinetic parameters for removal of indigo carmine dye.

Adsorption kinetic model	Equation	Parameter	Irradiated WEPS
Pseudo-first-order	$q_t = q_e(1 - e^{-k_1 t})$	q_e (mg/g)	13.76
		k_1 (min^{-1})	9.494
		R^2	0.986
		χ^2	0.226
		RSS	2.041
Pseudo-second-order	$q_t = \frac{q_e^2 k_2 t}{1 + q_e k_2 t}$	q_e (mg/g)	14.21
		k_2 (g/min·mg)	0.094
		R^2	0.994
		χ^2	0.095
		RSS	0.860

Fenton process. Moreover, it is well known that the H_2O_2 and the ferrous ions are more stable at a low pH. For example, at pH less than 2.0, the reaction between H_2O_2 and Fe^{2+} could be slowed down, because the H_2O_2 can probably remain stable by solvating a proton to form an oxonium ion (Eq. 2) (Nidheesh et al., 2013).



An advantage of this work was achieved decrease of the pH, from 6.7 (corresponding to the textile wastewater) to 3.2 for the resulting composite. Which is due to the acid nature of the sulfonated polystyrene. Therefore, pH = 3.2 was taken as reference, and no tests were carried out at different pH.

The effects of the H_2O_2 on the decolorization of the textile wastewater, are shown in Fig. 10. The H_2O_2 concentrations were 0.08, 0.16,

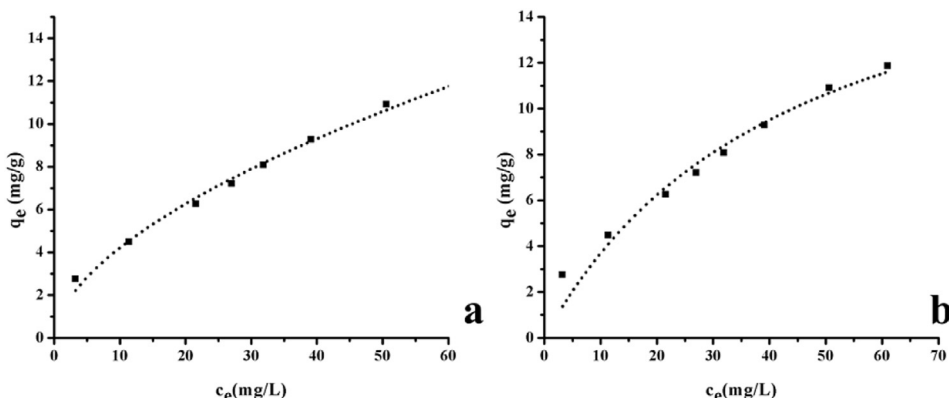


Fig. 9. Adsorption isotherms models: Freundlich (a), and Langmuir (b); adsorbent dose = 2 g/L, sample volume = 100 mL, and equilibrium time = 30 min.

Table 2
Adsorption isotherms parameters for removal of indigo carmine dye.

Adsorption isotherm models	Equation	Parameters	Irradiated WEPS
Langmuir	$q_e = \frac{q_{max}bC_e}{1 + bC_e}$	q_{max} (mg/g)	20.01
		b (L/g)	0.022
		R^2	0.955
Freundlich	$q_e = KFC_e^{1/n}$	KF (mg/g) (L/mg)	1.127
		$1/n$	0.475
		R^2	0.990
Langmuir-Freundlich	$q_e = \frac{KC_e^{1/n}}{1 + aC_e^{1/n}}$	K (mg/g)	16181.7
		a (L/g)	0.000069
		$1/n$	0.57
		R^2	0.989

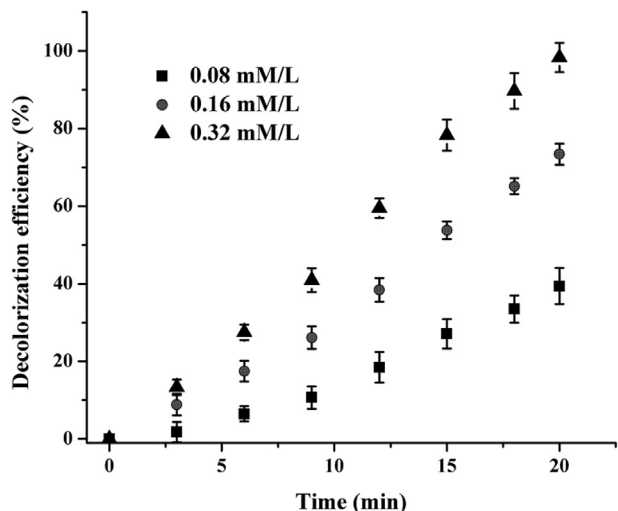


Fig. 10. Effect of the H_2O_2 concentrations on the decolorization of indigo carmine dye; [composite (FeO-NPs + iS-WEPS) = 2 g/L, pH = 3.2, t = 20 min].

0.32 mM/L. As it is shown, the indigo carmine dye degradation rate increase when increase H_2O_2 concentration. Moreover, maximum removal, namely 99%, was obtained for a concentration of 0.32 mM/L.

Removal of indigo carmine dye occurs on the surface of the composite (FeO-NPs + iS-WEPS) (the catalyst), after reacting with H_2O_2 . The removal follows Eqs. (3), (4), (5), and (6) (Araujo et al., 2011). The heterogeneous Fenton process shows several reactions on the catalyst surface, producing $HO\bullet$ and $HO_2\bullet$ radicals. High concentration of catalyst provoke that more H_2O_2 molecules reach the surface of the composite (FeO-NPs + iS-WEPS), and react with Fe^{2+} , resulting in a higher reaction rate. Thus, low H_2O_2 concentration means low oxidation rate. These

results are agree with those reported by (Babaei et al., 2017; Tai et al., 2016).



The current mechanism involves hydroxyl radical production, by means of the reactions between H_2O_2 and the iron oxides. Moreover, this can react with organic matter in the water through direct and indirect pathways. Mainly, by means of double bond addition, hydrogen abstraction or by electron-transfer reactions (Khan et al., 2017). Thus, the result is the elimination of organics up to their mineralization (Guivarch et al., 2003).

3.7.1. Removal of indigo carmine dye in textile wastewater

The removal percentage of the indigo carmine dye achieved by the composite (FeO-NPs + iS-WEPS) was 6% and by the H_2O_2 of 14%. Nevertheless, the combination of both following a Fenton process, achieved 99% of removal (Fig. 11a). The results show diminution of the chemical oxygen demand (COD) from 2,422 mg/L to 411 mg/L with a reaction time of 20 min (Fig. 11b), is to say a reduction of 83%. The high dye elimination was due to the reactive radicals produced in the Fenton process. Moreover, the complete dye removal does not always mean complete mineralization, because the textile wastewater are always a complex mixture of chemicals.

The results depend on the textile wastewater characteristics. Some studies concerning to dye removal show lower values than those obtained in this work. For example: a) Almazan et al., 2015, obtained 90% removal of indigo blue in more than 1 h, through of a Fenton process (Almazán-Sánchez et al., 2016), b) Subbulekshmi et al., 2107 developed the system (CuO + zeolite) and H_2O_2 ; the removal of indigo carmine dye was obtained in 1h, with a COD reduction of 80% (Subbulekshmi and Subramanian, 2017), c) in other study, Fe_2O_3 supported-zeolite was elaborated as a heterogeneous catalyst, for the degradation of indigo carmine, through Photo-Fenton process. The results show almost discoloration after 10 min (Moumni et al., 2018). These studies used prepared solutions. Unfortunately, there are few studies which using textile effluents or wastewater, because in such systems there are many variables to control.

Similar results for COD reduction were obtained with combined processes. For example: a) textile effluent treated with electro-Fenton, achieving a COD reduction of 86% (Roshini et al., 2017), b) textile wastewater by means of photo-Fenton process, with a COD reduction of 84% (Negueroles et al., 2017), c) Ultrasonic- Fenton processes for degradation of azo dye in textile wastewater, with a COD reduction of

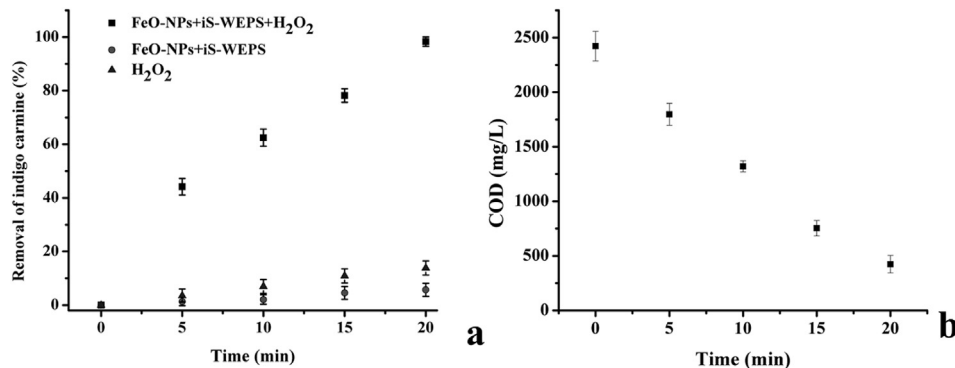


Fig. 11. Removal of indigo carmine dye in the textile wastewater (a), and COD produced through Fenton process (b); H_2O_2 = 0.32 mM/L, composite (FeO-NPs + iS-WEPS) = 2 g/L, pH = 3.2.

79.25%. Finally, a similar initial COD value (2,360 mg/L) obtained in this work was comparable to that reported by (Jaafarzadeh et al., 2018).

4. Conclusions

In this work, waste expanded polystyrene (WEPS) was submitted to gamma rays and to a sulfonation process for to improve the removal of indigo carmine dye in textile wastewater. According to the thermal characterization, T_g decrease for irradiated WEPS is produced by the decrease of its molecular weight, caused by the scissions of the polymer chains. Moreover, there are not evidences for changes in its chemical structure according to the FT-IR characterization. Nevertheless, an improvement of 50% was obtained for the degree of sulfonation of the WEPS irradiated at 200 kGy, in comparison with the non-irradiated ones.

After irradiation, the composites elaborated with (iS-WEPS), and iron oxide nanoparticles (FeO-NPs): a) had morphological changes, which increased their superficial area and the degree of hydrophilicity, such modification promoted the adsorption process; b) had better fitting with the pseudo-second order model, for the description of the adsorption kinetics; c) the adsorption occurred by chemisorption, with exchange of electrons between the composite and the indigo carmine dye; and d) they were used as a heterogeneous Fenton catalyst, and the elimination of the indigo carmine dye in textile wastewater increase when the H₂O₂ concentration increase. Finally, it was obtained 99% removal of indigo carmine, as well as 83% of COD reduction; according to the experimental conditions: H₂O₂ = 0.32 mM/L, composite = 2 g/L, pH = 3.2, and a reaction time of 20 min.

Declarations

Author contribution statement

Gonzalo Martínez-Barrera, Cristina de León-Condés, Gabriela Roa-Morales, Patricia Balderas-Hernández, Carmina Menchaca-Campos, Bryan Bilyeu, Fernando Ureña-Núñez, Helen Toledo: Conceived and designed the experiments; Performed the experiments; Analyzed and interpreted the data; Contributed reagents, materials, analysis tools or data; Wrote the paper.

Funding statement

This research did not receive any specific grant from funding agencies in the public, commercial, or not-for-profit sectors.

Competing interest statement

The authors declare no conflict of interest.

Additional information

No additional information is available for this paper.

Acknowledgements

Authors acknowledge academic support of the Facultad de Química-UAEM Mexico, and the CCIQS UAEM-UNAM Mexico institutions. To M. Alejandra Nuñez Pineda (CCIQS UAEM-UNAM) for running DSC analysis of the composites, Dr. Uvaldo Hernández Balderas, Dr. Alfredo Rafael Vilchis Néstor, and Dr. Fernando Romero Romero for technical support. One of the authors, De León-Condés acknowledges to Consejo Nacional de Ciencia y Tecnología de México (CONACYT), for the fellowships of Graduate Studies and Beca Mixta.

References

- Al-Sabagh, A.M., Moustafa, Y.M., Hamdy, A., Killa, H.M., Ghanem, R.T.M., Morsi, R.E., 2018. Preparation and characterization of sulfonated polystyrene/magnetite nanocomposites for organic dye adsorption. *Egypt. J. Pet.* 27, 403–413.
- Aljeboree, A.M., Alshirifi, A.N., Alkaim, A.F., 2017. Kinetics and equilibrium study for the adsorption of textile dyes on coconut shell activated carbon. *Arab. J. Chem.* 10, S3381–S3393.
- Almazán-Sánchez, P.T., Solache-Ríos, M.J., Linares-Hernández, I., Martínez-Miranda, V., 2016. Adsorption-regeneration by heterogeneous Fenton process using modified carbon and clay materials for removal of indigo blue. *Environ. Technol.* 37, 1843–1856.
- Araujo, F.V.F., Yokoyama, L., Teixeira, L.A.C., Campos, J.C., 2011. Heterogeneous Fenton process using the mineral hematite for the discoloration of a reactive dye solution. *Braz. J. Chem. Eng.* 28, 605–616.
- Babaei, A.A., Kakavandi, B., Rafiee, M., Kalantarhormizi, F., Purkaram, I., Ahmadi, E., Esmaeili, S., 2017. Comparative treatment of textile wastewater by adsorption, Fenton, UV-Fenton and US-Fenton using magnetic nanoparticles-functionalized carbon (MNP@C). *J. Ind. Eng. Chem.* 56, 163–174.
- Babuponnusami, A., Muthukumar, K., 2012. Advanced oxidation of phenol: a comparison between Fenton, electro-Fenton, sono-electro-Fenton and photo-electro-Fenton processes. *Chem. Eng. J.* 183, 1–9.
- Blanco-Flores, A., Colín-Cruz, A., Gutiérrez-Segura, E., Sánchez-Mendieta, V., Solís-Casados, D.A., Garrudo-Guirado, M.A., Batista-González, R., 2014. Efficient removal of crystal violet dye from aqueous solutions by vitreous tuff mineral. *Environ. Technol.* 35, 1508–1519.
- Blanco-Flores, A., Colín-Cruz, A., Gutiérrez-Segura, E., Vilchis-Nestor, A., 2016. Removal of malachite green dye from aqueous solution through inexpensive and easily available tuffite, bentonite and vitreous tuff minerals. *Revista Latinoamericana de Recursos Naturales* 12, 1–17.
- Coreño-Alonso, J., Mendez-Bautista, T., 2010. Relationship between structure and properties of polymers. *Educ. Quím.* 21, 291–299.
- Crane, R.A., Scott, T.B., 2012. Nanoscale zero-valent iron: future prospects for an emerging water treatment technology. *J. Hazard Mater.* 211–212, 112–125.
- Cui, H., Liu, Y., Ren, W., 2013. Structure switch between α -Fe₂O₃, γ -Fe₂O₃ and Fe₃O₄ during the large scale and low temperature sol-gel synthesis of nearly monodispersed iron oxide nanoparticles. *Adv. Powder Technol.* 24, 93–97.
- De León-Condés, C.A., Roa-Morales, G., Martínez-Barrera, G., Balderas-Hernández, P., Menchaca-Campos, C., Ureña-Núñez, F., 2019. A novel sulfonated waste polystyrene/iron oxide nanoparticles composite: green synthesis, characterization and applications. *J. Environ. Chem. Eng.* 7, 102841.
- Domenech, X., Jardim, W.F., Litter, M.I., 2004. Procesos avanzados de oxidación para la eliminación de contaminantes. In: *Eliminación de Contaminantes Por Fotocatálisis Heterogénea*. CIEMAT, Madrid, p. 388.
- Espinosa, J.C., Catalá, C., Navalón, S., Ferrer, B., Álvaro, M., García, H., 2018. Iron oxide nanoparticles supported on diamond nanoparticles as efficient and stable catalyst for the visible light assisted Fenton reaction. *Appl. Catal. B Environ.* 226, 242–251.
- Fahmy, H.M., Mohamed, F.M., Marzouq, M.H., Mustafa, A.B.E.D., Alsoudi, A.M., Ali, O.A., Mohamed, M.A., Mahmoud, F.A., 2018. Review of green methods of iron nanoparticles synthesis and applications. *Bionanoscience* 8, 491–503.
- Grisales, C.M., Salazar, L.M., Garcia, D.P., 2019. Treatment of synthetic dye baths by Fenton processes: evaluation of their environmental footprint through life cycle assessment. *Environ. Sci. Pollut. Control Ser.* 26, 4300–4311.
- Guivar, J.A.R., Martínez, A.I., Anaya, A.O., Valladares, L.D.L.S., Félix, L.L., Domínguez, A.B., 2014. Structural and magnetic properties of monophasic maghemite (γ -Fe₂O₃) nanocrystalline powder. *Adv. Nanoparticles* 03, 114–121.
- Guivarch, E., Trevin, S., Lahitte, C., Oturan, M.A., 2003. Degradation of azo dyes in water by Electro-Fenton process. *Environ. Chem. Lett.* 1, 38–44.
- Gutiérrez-Segura, E., Solache-Ríos, M., Colín-Cruz, A., 2009. Sorption of indigo carmine by a Fe-zeolitic tuff and carbonaceous material from pyrolyzed sewage sludge. *J. Hazard Mater.* 170, 1227–1235.
- Hartmann, M., Kullmann, S., Keller, H., 2010. Wastewater treatment with heterogeneous Fenton-type catalysts based on porous materials. *J. Mater. Chem.* 20, 9002–9017.
- Haryono, A., Harmami, S.B., 2012. Sulfonation of waste high impact polystyrene from food packaging as a polymeric flocculant. *Adv. Mater. Res.* 486, 426–431.
- Holkar, C.R., Jadhav, A.J., Pinjari, D.V., Mahamuni, N.M., Pandit, A.B., 2016. A critical review on textile wastewater treatments: possible approaches. *J. Environ. Manag.* 182, 351–366.
- Jaafarzadeh, N., Takdastan, A., Jorfi, S., Ghanbari, F., Ahmadi, M., Barzegar, G., 2018. The performance study on ultrasonic/Fe₃O₄/H₂O₂ for degradation of azo dye and real textile wastewater treatment. *J. Mol. Liq.* 256, 462–470.
- Khan, S., He, X., Khan, J.A., Khan, H.M., Boccelli, D.L., Dionysiou, D.D., 2017. Kinetics and mechanism of sulfate radical- and hydroxyl radical-induced degradation of highly chlorinated pesticide lindane in UV/peroxymonosulfate system. *Chem. Eng. J.* 318, 135–142.
- Liu, J., Wong, L.M., Gurudayal Wong, L.H., Chiam, S.Y., Yau Li, S.F., Ren, Y., 2016. Immobilization of dye pollutants on iron hydroxide coated substrates: kinetics, efficiency and the adsorption mechanism. *J. Mater. Chem.* 4, 13280–13288.
- Liu, X., Yin, H., Lin, A., Guo, Z., 2017. Effective removal of phenol by using activated carbon supported iron prepared under microwave irradiation as a reusable heterogeneous Fenton-like catalyst. *J. Environ. Chem. Eng.* 5, 870–876.
- Moumni, C., Fakhfakh, N., Hadjltaief, H.B., Benzina, M., 2018. Response surface methodology optimization of heterogeneous catalyst Fe₂O₃-zeolite synthesis for the discoloration of indigo carmine dye by photo-fenton process. In: Khélifi, A.K.K.B.D. (Ed.), *Advances in Science, Technology & Innovation (IEREK Interdisciplinary Series for Sustainable Development)*. Springer, Cham, pp. 1109–1111.

- Negueroles, P., Bou Belda, E., Santos Juanes, L., Amat, A., Vercher, R., Monllor, P., Vicente, R., 2017. Treatment and reuse of textile wastewaters by mild solar photo-Fenton in the presence of humic-like substances. *Environ. Sci. Pollut. Control Ser.* 24, 12664–12672.
- Nidheesh, V., Gandhimathi, R., Ramesh, T., 2013. Degradation of dyes from aqueous solution by Fenton processes: a review. *Environ. Sci. Pollut. Control Ser.* 20, 2099–2132.
- Olmos, D., Martín, E.V., González-Benito, J., 2014. New molecular-scale information on polystyrene dynamics in PS and PS-BaTiO₃ composites from FTIR spectroscopy. *Phys. Chem. Chem. Phys.* 16, 24339–24349.
- Pandey, B.K., Shahi, A.K., Shah, J., Kotnala, R.K., Gopal, R., 2014. Optical and magnetic properties of Fe₂O₃ nanoparticles synthesized by laser ablation/fragmentation technique in different liquid media. *Appl. Surf. Sci.* 289, 462–471.
- Roshini, P.S., Gandhimathi, R., Ramesh, S.T., Nidheesh, P.V., 2017. Combined electro-fenton and biological processes for the treatment of industrial textile effluent: mineralization and toxicity analysis. *J. Hazard. Toxic. Radioact. Waste* 21, 04017016.
- Sanmuga, P.E., Senthamil, S.P., 2017. Water hyacinth (*Eichhornia crassipes*) – an efficient and economic adsorbent for textile effluent treatment – a review. *Arab. J. Chem.* 10, S3548–S3558.
- Shahwan, T., Abu Sirriah, S., Nairat, M., Boyaci, E., Eroglu, A.E., Scott, T.B., Hallam, K.R., 2011. Green synthesis of iron nanoparticles and their application as a Fenton-like catalyst for the degradation of aqueous cationic and anionic dyes. *Chem. Eng. J.* 172, 258–266.
- Spadaro, G., Alessi, S., Dispenza, C., 2017. Ionizing radiation-induced crosslinking and degradation of polymers. In: Sun, Y., Chmielewski, Andrzej G. (Eds.), *Applications of Ionizing Radiation in Materials Processing*. INTECH, Italy, pp. 167–182.
- Subbulekshmi, N.L., Subramanian, E., 2017. High degree Fenton-like catalytic activity of CuO/zeolite X catalyst from coal fly ash in mineralization of Indigo Carmine dye. *J. Environ. Biotechnol. Res.* 6, 228–237.
- Tabekh, H., Hassan, M., Kurdi, A., Ajji, Z., 2015. Sulphonation of expanded polystyrene waste with commercial sulphuric acid for potential use in removal of heavy metals from contaminated waters. *Polimeri: časopis za plastiku i gumu* 36, 1-2:11-14.
- Tai, C., She, J., Yin, Y., Zhao, T., Wu, L., 2016. Degradation of 2,4,6-trichlorophenol using hydrogen peroxide catalyzed by nanoscale zero-valent iron supported on ion exchange resin. *J. Nanosci. Nanotechnol.* 16, 5850–5855.
- Wang, T., Lin, J., Chen, Z., Megharaj, M., Naidu, R., 2014. Green synthesized iron nanoparticles by green tea and eucalyptus leaves extracts used for removal of nitrate in aqueous solution. *J. Clean. Prod.* 83, 413–419.
- Yabagi, J.A., Kimpa, M.I., Muhammad, M.N., Rashid, S. Bin, Zaidi, E., Agam, M.A., 2018. The effect of gamma irradiation on chemical, morphology and optical properties of polystyrene nanosphere at various exposure time. *IOP Conf. Ser. Mater. Sci. Eng.* 298.
- Yousif, E., Haddad, R., 2013. Photodegradation and photostabilization of polymers, especially polystyrene: Review. *SpringerPlus* 2, 1–32.
- Yu, B., Li, Z., Cong, H., Li, G., Peng, Q., Yang, C., 2017. Synthesis and application of sulfonated polystyrene/ferrosoferric oxide/diazo resin nanocomposite microspheres for highly selective removal of dyes. *Mater. Des.* 135, 333–342.
- Zaidi, S.M.J., 2003. Polymer sulfonation – a versatile route to prepare proton-conducting membrane material for advanced technologies. *Arabian J. Sci. Eng.* 28, 183–194.
- Zaied, M., Chutet, E., Peulon, S., Bellakhal, N., Desmazières, B., Dachraoui, M., Chaussé, A., 2011. Spontaneous oxidative degradation of indigo carmine by thin films of birnessite electrodeposited onto SnO₂. *Appl. Catal. B Environ.* 107, 42–51.